



# Improvement of oxidation resistance of TiAl6V4 alloy by siliconizing from liquid phase using melts with high silicon content

T. Kubatík\*, M. Jáglová, E. Kalabisová, V. Číhal

SVUOM s.r.o., V Šáreckém údolí 2329, Praha, Czech Republic

## ARTICLE INFO

### Article history:

Received 7 February 2010  
Received in revised form 9 February 2011  
Accepted 11 February 2011  
Available online 22 February 2011

### Keywords:

Silicides  
Aluminides  
High temperature oxidation  
Liquid-phase siliconizing  
Coating

## ABSTRACT

This work deals with a study of properties of layers prepared by a simple, cheap, and efficient method of siliconizing from liquid phase. They were prepared using the melts AlSi20 and AlSi28 (wt.%); their high silicon content provides for almost a twofold rate of the layers formation. Main component of the layers formed by siliconizing is  $\tau_2$  – phase  $[\text{Ti}(\text{Al}_x\text{Si}_{1-x})]$ , where  $x = 0.15\text{--}0.3$ . This phase is also formed in aluminium melts containing 5 and 10 wt.% of silicon, as documented in [1–4]. The growth rate of silicide–aluminide layers is a parabolic function; the rate constant for melts AlSi20 and AlSi28 expressed in  $\text{m}^2/\text{s}$  was determined as:

$$k_{\text{AlSi20}} = 22.344 \exp\left(\frac{-227,412.8}{RT}\right) \text{ and } k_{\text{AlSi28}} = 7,936,635 \exp\left(\frac{-329,741}{RT}\right).$$

This equation is valid under experimental conditions. The protective layers with a high silicon content are particularly suitable for high-temperature applications as they contain thermodynamically stable phases, such as  $\text{TiSi}_2$ ,  $\text{SiO}_2$  and  $\text{Al}_2\text{O}_3$  creating an efficient barrier against diffusion of oxygen and nitrogen. The protective effect of these layers was studied by cyclic oxidation at temperatures 1123 and 1223 K. These layers rich in silicide–aluminide phase have been proved to provide, in spite of their inhomogeneity, for excellent protection of the titanium alloy against high-temperature oxidation.

© 2011 Elsevier B.V. All rights reserved.

## 1. Introduction

Using of titanium alloys in a high-temperature environment is mainly limited by its considerable high-temperature oxidation; it is reported to be technically acceptable up to maximum temperature of 550 °C [5,6].

One way of improving oxidation resistance is alloying of titanium with elements such as silver, tungsten, niobium, aluminium, silicon, etc. [7–12]. Many works have been published in which authors studied effects of these alloying elements on increasing the oxidation resistance. However, alloying induces changes in mechanical properties, above all loss of toughness. In order to maintain these properties, surface alloying is sometimes chosen, such as, for instance, ion implantation, plasma injections, cementation, laser surface treatment, PVD, and others [13,14]. The surface alloying by the mentioned method utilizes in particular aluminium, molybdenum, niobium, tungsten, and silicon [15]. Silicon forms silicides that make a very efficient protective barrier against diffusion of oxygen during high-temperature oxidation [16–23]. The protective layers based on silicide–aluminium phases can be formed

by the method of siliconizing from liquid phase [24–28] by dipping titanium and titanium alloys into the Al–Si melt. They have a marked effect on increasing the high-temperature oxidation resistance based on formation of oxides  $\text{SiO}_2$  and  $\text{Al}_2\text{O}_3$  that obstruct oxygen diffusion to the surface of the base metal, as documented by several authors [2–4,27,28].

The siliconizing from liquid phase is a very efficient and cheap method of forming a protective layer on TiAl6V4; it has been proved that using of melts with a high silicon content has an effect on the rate of its formation.

Generally, the growth rate of layers is a parabolic function

$$y_i^2 = k_i t, \quad (1)$$

where  $y$  is thickness of layer  $i$ ,  $k_i$  is rate constant, and  $t$  is exposition time in siliconizing.

The rate constant  $k_i$  valid for layer  $i$  is defined by the Arrhenius equation:

$$k_i = A \exp\left(\frac{-Q}{RT}\right), \quad (2)$$

where  $A$  is coefficient,  $Q$  activation energy,  $R$  gas constant, and  $T$  absolute temperature. Chemical composition showed as much as 50% silicon content in the layer, which is a prerequisite of excellent protective effects in high-temperature oxidation.

\* Corresponding author. Tel.: +420 235355851; fax: +420 235355854.  
E-mail address: [kubatik@svuom.cz](mailto:kubatik@svuom.cz) (T. Kubatík).

## 2. Experimental

Titanium (Grade 2) and the titanium alloy TiAl6V4 (Grade 5) were used in the experiments. The samples were of cylindrical shape of diameter 10 mm and length 6 mm. The samples for layers preparation were ground on SiC papers to coarseness P-1200 and polished with a diamond paste of granularity 5 and 1  $\mu\text{m}$ . The samples were then degreased using acetone in an ultrasound bath and air-dried. The melt was prepared from pure aluminium (99.5 wt.% Al) and silicon (5 N). Aluminium was melted in a graphite crucible placed in an electric resistance furnace. After adding pieces of silicon and their dissolving in the melt, the content of the crucible was mixed with a graphite rod and kept at temperature of 1073 K for 30 min. Melts containing 20 and 30% by weight of silicon were prepared. The samples intended for depositing the layers were placed into the melt at the crucible bottom. After 5 min, they were taken out using pliers and cooled down in the air. The layers were inspected using an electron scanning microscope TESCAN VEGA fitted with an EDX analyzer for chemical microanalyses of the surface layers. The samples were imbedded into a resin, ground with SiC paper of coarseness P-180 to P-1200, polished with a diamond paste of granularity 5 and 1  $\mu\text{m}$ . Thickness of individual layers was measured by SEM. Average thickness of the layers was obtained by measuring thickness of layers at ten different points.

The samples for oxidation experiments were prepared by etching the stuck-on solidified melt in 10% HCl and leaving them in the acid until all residues of the stuck-on solidified melt have been removed. After being taken out from the acid, the samples were cleaned with a brush in distilled water and dried in the air. Cyclic oxidation was accomplished in the electric resistance furnace at 1123 and 1223 K for 204 h together with the samples of titanium and the titanium alloy TiAl6V4 without layers. One cycle includes 12-h exposition in the furnace with laboratory atmosphere at constant temperature, subsequent quick cooling to laboratory temperature, and weighing. Scale fallen off from the sample during oxidation was added to the total sample weight.

## 3. Results

### 3.1. Microstructure of layers

Fig. 1 shows SEM scans of cuts of the layers prepared by siliconizing in liquid phase at 1073 K for 5 min in the melts AlSi20 (a) and AlSi28 (b). The layers of approximate thickness 121  $\mu\text{m}$  and 227  $\mu\text{m}$  were prepared in the melts AlSi20 and AlSi28, respectively.

The layers consist of silicide–aluminide particles of composition 15–27% Al, 44–54% Si, and about 0.7–1% V; the inter-dendritic space is filled with aluminium. This particle composition corresponds to the  $\tau_2$ -phase referred to in other works as the main product of siliconizing from liquid phase. In Fig. 1 they can be seen as light grey particles. The inter-particle space is filled with pure aluminium – dark field between the phases. Results of the chemical analysis related to the samples in Fig. 1 are shown in Table 1. The results correspond to thermodynamic description as well as to results of other works dealing with siliconizing from liquid phase [24]. Using of the melts with a high silicon content results in formation of the layers rich in silicon (up to 52% Si).

**Table 1**

The EDX analysis results of micro-zones marked in Fig. 1(a) and (b), [compositions at.%].

Micro-zone	Ti	Al	Si	V	Main phases
Area-1	30.92	15.99	52.37	0.72	$\tau_2$ -phase + Al
Area-2	25.07	29.99	48.89	0.95	$\tau_2$ -phase + Al
Area-3	28.27	22.53	48.29	0.91	$\tau_2$ -phase
Area-4	29.73	15.26	54.01	1.00	$\tau_2$ -phase + Al
Area-5	21.74	35.47	41.96	0.82	$\tau_2$ -phase + Al
Area-6	21.80	32.94	44.35	0.92	$\tau_2$ -phase

### 3.2. Kinetics of layer growth

It follows from our experiments as well as from works of other authors [13,24,25] that, with the same temperatures and reaction times, higher silicon content in the melt significantly increases the growth rate of the layers. A layer of thickness 231.1  $\mu\text{m}$  is formed in the melt AlSi20 during 10-min exposition; whereas, almost a twice as thick layer 507.6  $\mu\text{m}$  is formed in the melt AlSi28 during the same time. The results of measuring the layer thickness are summarized in the graph in Fig. 2. Using regression analysis, activation energies  $Q = -2.344 \text{ kJ/mol}$  and  $Q = -329,741 \text{ kJ/mol}$  were obtained for the melt AlSi20 and AlSi28, respectively. The lines in the graph in Fig. 3 can be described by the equations:

$$k_{\text{AlSi20}} = 22.344 \exp \left( \frac{-227,412.8}{RT} \right) \quad (3)$$

$$k_{\text{AlSi30}} = 7,936,635 \exp \left( \frac{-329,741}{RT} \right) \quad (4)$$

The dependence of thickness of the silicide–aluminide layers (expressed in m) on the siliconizing time and temperature can be described by the equations:

$$y_{\text{AlSi20}}^2 = 22.344 \exp \left( \frac{-227,412.8}{RT} \right) t \quad (5)$$

$$y_{\text{AlSi30}}^2 = 7,936,635 \exp \left( \frac{-329,741}{RT} \right) t \quad (6)$$

### 3.3. Oxidation resistance

Oxidation resistance was assessed as dependence of weight gain on time. Weight of the fallen off scale was included into the total weight increment. Oxidation resistance of the layers was compared with that of pure titanium and the most often used titanium alloy TiAl6V4. In our previous experiments, we found the most

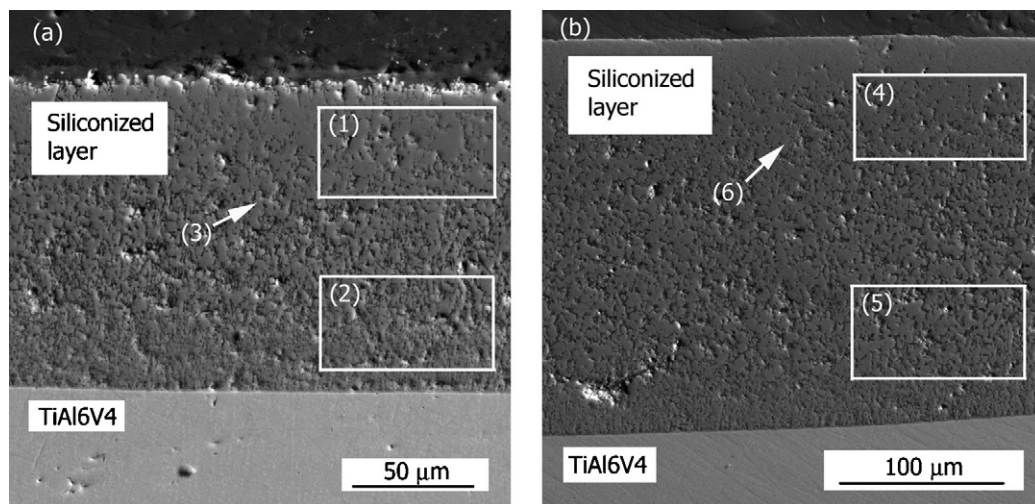


**Fig. 1.** SEM micrographs of the cross section surface layers prepared (a) AlSi20, (b) AlSi28.

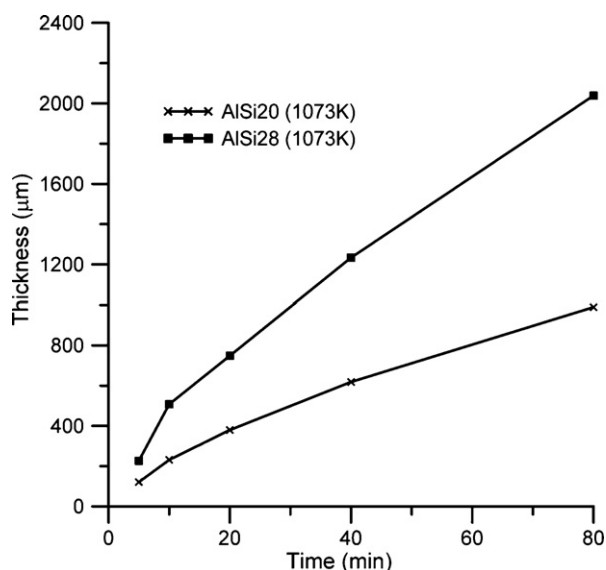


Fig. 2. Kinetics of growth of layers in the melts AlSi20 and AlSi28 at temperature 1073 K.

significant effect of the protective layers at the temperature of 1123 K. At lower temperatures (1023 K), no significant difference in the effect of protective layers was found. At high temperatures (1223 K), partial destruction of the prepared layers was observed within relatively short time. The results of the oxidation experiments at temperature of 1123 K are graphically depicted in Fig. 4. The graph clearly shows that the layers sharply increase the oxidation resistance for the whole time of the experiment (204 h). At exposition exceeding 50 h, the weight increment approaches zero. A difference can be observed in the value of gain for the layers prepared from different melts: the layer prepared in the melt AlSi28 has lower weight gain ( $0.00778 \text{ g/cm}^2$ , 204 h) compared with the layer prepared in the melt AlSi20 ( $0.0118 \text{ g/cm}^2$ , 204 h). This difference is mainly caused by a great difference in thickness of the layers. High oxidation rate found in titanium and in the alloy TiAl6V4 follows a parabolic dependence. The weight gain of the alloy TiAl6V4 ( $0.166 \text{ g/cm}^2$ , 204 h) are almost 21-times higher than those for the sample covered with the layer prepared in the melt AlSi28. The layers were also tested at the oxidation temperature 1223 K. This temperature is already too high and a considerable destruction of all samples was observed. The results of the high-temperature oxidation are shown in the graph in Fig. 5. Glassy scale was formed on the titanium surface during oxidation; it was stuck to the corundum crucible and the measurement was terminated after 36 h. Similarly,

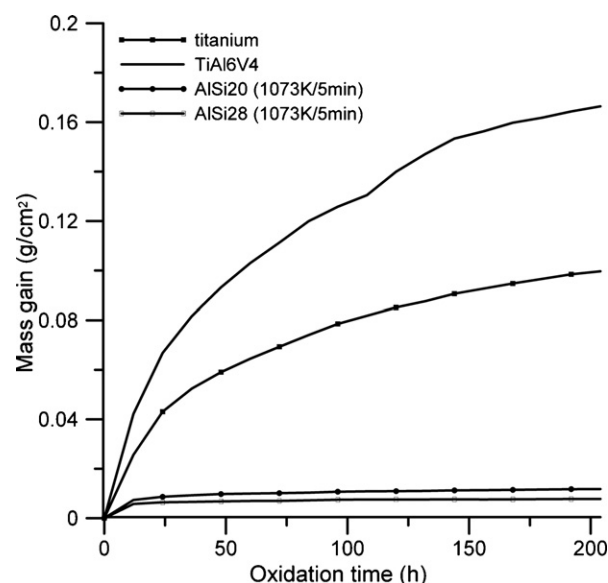


Fig. 4. Cyclic oxidation of samples with protective layers, alloy TiAl6V4 and Ti at 1123 K.

the alloy TiAl6V4 did not form compact scale which was falling off. The final weight increment was  $0.209 \text{ g/cm}^2$  during 204 h. It is obvious that the protective layers markedly reduce the oxidation rate and up to about 108 h the weight gain are uniform. After this period, the oxidation rate increases. In case of the layer prepared in the melt AlSi28, the oxidation rate is dramatically increased; the final weight increment is  $0.0425 \text{ g/cm}^2$  in 204 h, a value almost 5-times lower.

### 3.4. Microstructures of layers after oxidation

Microstructure of cross section the layers after oxidation was studied using the electron microscope. Fig. 6a shows the cross section the titanium layer oxidized at 1123 K for 204 h. It is apparent from the figure that cyclic oxidation has an adverse effect on formation of the protective layer on titanium and the alloy TiAl6V4. The oxide layer is composed of individual observable layers; they do not form a compact solid layer but a layer formed of many pores of total

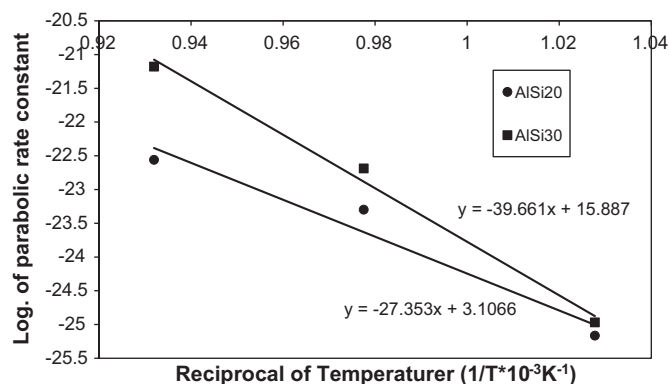


Fig. 3. Arrhenius plot for the parabolic rate constant of the growth of the silicide–aluminide coatings (silicizing alloy: AlSi20, AlSi28).

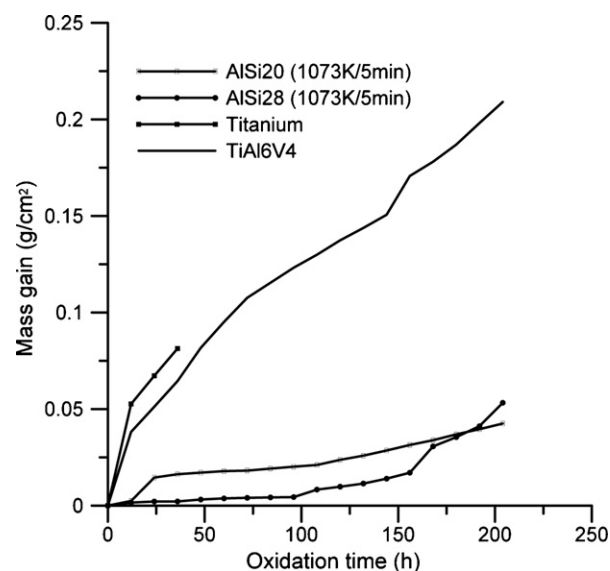
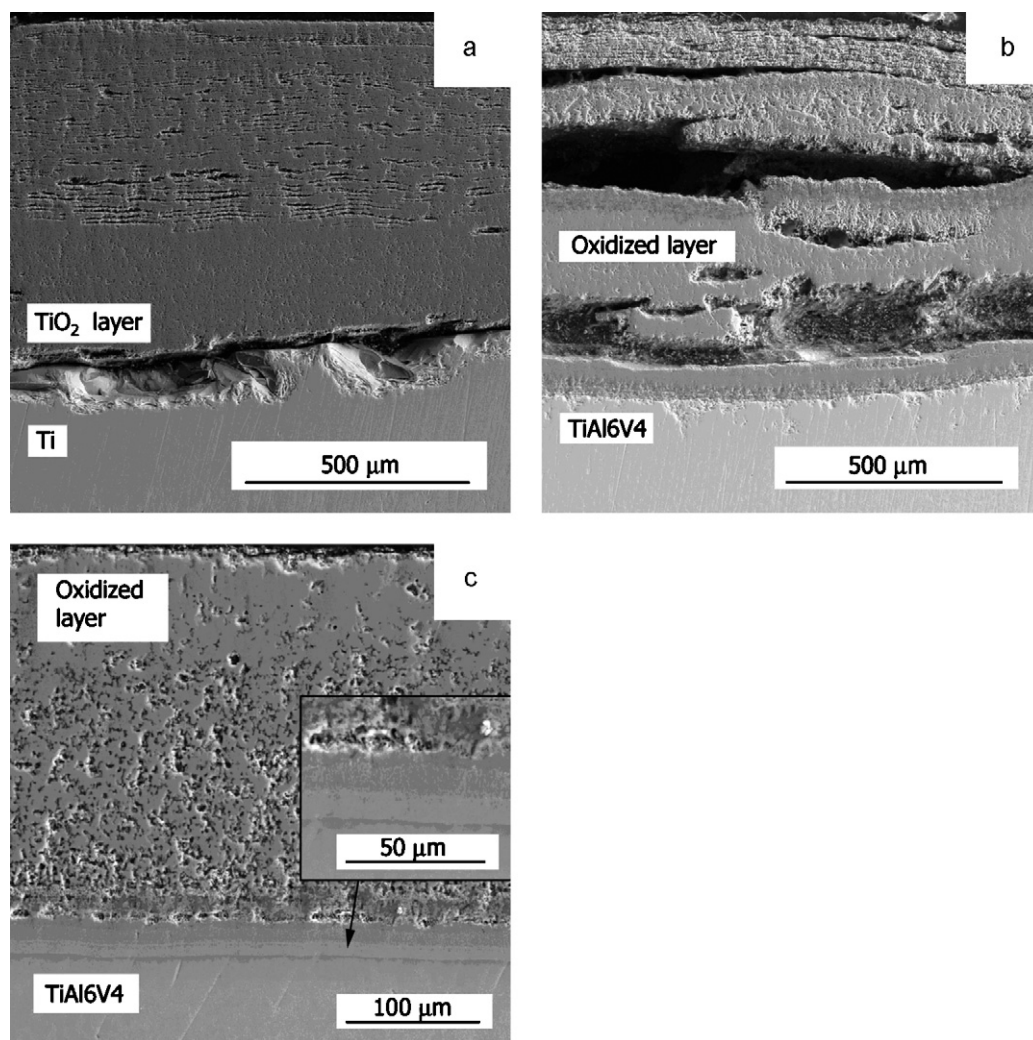


Fig. 5. Cyclic oxidation samples with protective layers, alloy TiAl6V4 and Ti at 1223 K.





**Fig. 6.** (a) SEM of cut of the oxidized layer on titanium at 1123 K, 204 h; (b) on the alloy TiAl6V4 at 1123 K, 204 h; (c) of cut of the layer prepared in the melt AlSi28, after oxidation at 1123 K, 204 h; detail of the layer-substrate interface.

thickness about 750 μm. However, nor does the alloy TiAl6V4 form a compact protective oxide layer that would protect the substrate at high temperatures. Fig. 6b shows that the layer is composed of several sub-layers with great pores in between that probably resulted from great thermal changes during respective oxidation cycles with approximate temperature gradient of 18 K/s. Fig. 6c shows the layer prepared in the melt AlSi28 after oxidation at 1123 K. It is apparent from the figure that no degradation of the protective layers takes place and the thermal cycles have no effect on the change in the layers microstructure. At high temperatures chemical changes occur in the layers. The original structure of the layer formed of the  $\tau_2$ -phase and aluminium in the inter-dendritic space was changed. Other experiments have also shown that aluminium in the layer diffuses to the surface where it oxidizes. Its content and the layer porosity are thus reduced. The content of aluminium in the  $\tau_2$ -phase also decreases. Based on the results of chemical analyses, it can be stated that phases of higher thermodynamic stability are formed, above all TiSi<sub>2</sub> [24] with a low to almost zero aluminium content. Inspection of the layer after oxidation shows that two sub-layers and a diffusion interface are formed at the substrate-layer interface, see the detail in Fig. 6c. These sub-layers are composed of mutually immiscible phases greatly differing in the aluminium content. Composition of the light sub-layer: 17.5% Al, 48.9% Si, 32% Ti, and 1.3% V. Composition of the dark sub-layer: 59% Al, 14% Si,

25% Ti, and 1.06% V (at.%). It can be expected that this interface will considerably hamper diffusion of oxygen to the substrate. The pores and cracks formed during layers preparation are sealed during this process and oxidation is reduced, as shown in the graph in Fig. 4; here, almost no weight increment was found after 50 h, which can probably be attributed to this phenomenon. It can be stated that, during the exposition time of up to 50 h, the observed quick increase was mainly caused by diffusion and oxidation of aluminium on the layer surface and by slow sealing of pores due to formation of Al<sub>2</sub>O<sub>3</sub>. Some results have shown that aluminium diffuses to the layer surface and the holes created in the structure provide for quite easy penetration of oxygen and nitrogen. In these cases, function of a protective barrier can be mainly attributed to the formed sub-layers. After oxidation at temperature of 1223 K 204 h, microstructure of cross section the layer prepared in the melt AlSi20 was studied using the electron microscope. Fig. 7 shows the layer after oxidation. The layer is flaked off and a relatively solid layer composed mainly of TiO<sub>2</sub> with a small content of silicon was formed between the original layer and the substrate during oxidation. The details show that the layer mainly consists of the TiSi<sub>2</sub> phase, which corresponds to the analysis. The original protective layer is formed of the phase TiSi<sub>2</sub>, the TiO<sub>2</sub> particles, and also of the original  $\tau_2$ -phase with a lower aluminium content of about 6% (at.) (see the results of chemical microanalysis). The layer thick-

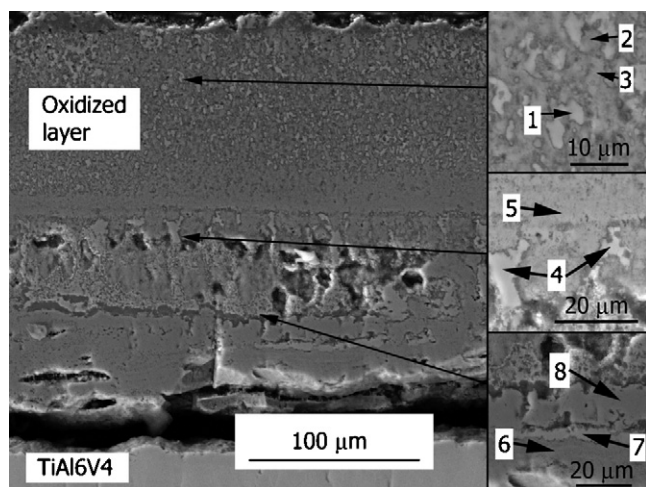


Fig. 7. SEM of cut of the layer prepared in the melt AlSi20, after oxidation at 1223 K, 204 h, details in the layer.

ness is approximately 220  $\mu\text{m}$ . Fig. 8 shows microstructure of cross section the layer prepared in the melt AlSi28 cut after oxidation at 950 °C/204 h. This layer was also flaked off and the substrate was quickly oxidized, as it is apparent from results in Table 2 where, in addition to results of the analyses, the phases present are also stated. Thickness of the layer thus formed is 430  $\mu\text{m}$ . The original layer consists of the  $\tau_2$ -phases with a lower content of aluminium which, in this case, diffused to the surface with formation of  $\text{Al}_2\text{O}_3$ . The rate of its diffusion is probably high thanks to the fact that at high temperatures aluminium is present in the liquid state. The detail of microstructure of the  $\text{TiO}_2$  layer shows that the  $\tau_2$ -phases with a small aluminium content and also the  $\text{TiSi}_2$  phases are enclosed inside the layer. The spot microanalysis also indicates that the substrate contains nitrogen that probably penetrated into the structure after flaking off of the originally stuck-on protective layer, which confirms presence of silicon. Fig. 9 presents an element map of the layer (AlSi28) cut after oxidation at 1223 K. It can be seen that aluminium diffuses to the surface where it forms a compact  $\text{Al}_2\text{O}_3$  layer. Oxygen is present uniformly in the whole layer width; at the surface, it is predominantly present as a com-

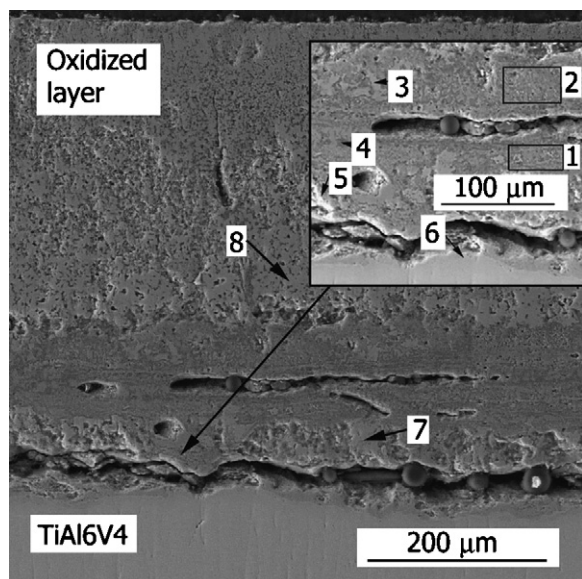


Fig. 8. SEM of cut of the layer prepared in the melt AlSi28, after oxidation at 1223 K, 204 h, detail of the layer-substrate interface.

Table 2

The EDX analysis results of micro-zones marked in Figs. 9 and 10 [composition at.%].

Micro-zone	O	Ti	Al	Si	V	Main phases
1. Fig. 9		34.79	1.85	61.75	1.62	$\text{TiSi}_2$
2. Fig. 9		67.01	12.99	17.82	2.18	$\tau_2$ -phase
3. Fig. 9		32.03	62.53	3.15	2.29	$\tau_2$ -phase
4. Fig. 9		31.19		67.07	1.74	$\text{TiSi}_2$
5. Fig. 9	Present	88.38	4.51	5.53	1.58	$\text{TiO}_2 + \text{Al}_2\text{O}_3 + \text{SiO}_2$
6. Fig. 9	Present	87.68		10.42	1.90	$\text{TiO}_2 + \text{SiO}_2$
7. Fig. 9		32.89		66.21	0.90	$\text{TiSi}_2$
8. Fig. 9	Present	96.39		3.61		$\text{TiO}_2 + \text{SiO}_2$
Area-1. Fig. 10	Present	71.03	2.39	24.41	2.19	$\text{TiO}_2 + \text{SiO}_2 + \text{Al}_2\text{O}_3$
Area-2. Fig. 10	Present	48.91	17.35	31.65	2.09	$\text{TiO}_2 + \text{SiO}_2 + \text{Al}_2\text{O}_3$
3. Fig. 10		32.35		66.73	0.91	$\text{TiSi}_2$
4. Fig. 10	Present	76.62	19.86	3.52		$\text{TiO}_2 + \text{Al}_2\text{O}_3 + \text{SiO}_2$
5. Fig. 10		32.46		66.51	1.03	$\text{TiSi}_2$
6. Fig. 10		82.5	5.84	9.69	1.97	Substrate + Si + N
7. Fig. 10	Present	76.62	19.86	3.52		$\text{TiO}_2 + \text{Al}_2\text{O}_3 + \text{SiO}_2$
8. Fig. 10		27.04	11.00	60.25	1.71	$\tau_2$ -phase

pact  $\text{Al}_2\text{O}_3$  layer; and at the interface layer-substrate it is mainly present in the form of  $\text{TiO}_2$ , which complies with results of the spot microanalysis. Silicon is non-uniformly dispersed in the layer; its highest concentration was found in the rutile layer between the original layer and the substrate. Thanks to aluminium diffusion to the layer surface, localities are formed where the  $\text{TiSi}_2$  particles are present.

#### 4. Discussion

The evaluation of the protective layers in the alloy TiAl6V4 prepared by the method of siliconizing from liquid phase using two types of melts with different silicon content – AlSi20 and AlSi28 has shown that high silicon content has no effect on change and chemical composition of the layers but has a significant effect on the rate of their growth. Using of the melt with higher silicon content (AlSi28) results in formation of the layer of almost a double thickness. It is obvious that a very short alloying with silicon provides compact protective layers. The chemical microanalysis has confirmed presence of the  $\tau_2$ -phase [Ti(Al<sub>x</sub>Si<sub>1-x</sub>)], where  $x=0.15-0.3$ ]. Growth rate of the layer is a parabolic function. Under the experimental conditions, the rate constants  $k_{\text{AlSi20}} = 22,344 \exp(-227,412.8/\text{RT}) \text{ m}^2/\text{s}$  and  $k_{\text{AlSi28}} = 7,936,635 \exp(-329,741/\text{RT}) \text{ m}^2/\text{s}$  have been found in the melts AlSi20 and AlSi28, respectively. Very short time allows preparation of the layers on the alloy TiAl6V4 without any influence on thermal treatment of the original substrate. Results of the cyclic high-temperature oxidation show that the prepared layers protect the substrate quite efficiently. At 1123 K, the weight gain caused by oxidation are almost non-detectable in both cases. In case of the melt AlSi28 after 204 h, the weight increment is 0.00778 g/cm<sup>2</sup>; in case of the alloy TiAl6V4 without a protective layer it is 0.166 g/cm<sup>2</sup> – almost 21-times more. The temperature of oxidation 1223 K is already too high with regard to practical applications of these layers; this is demonstrated by the results – the oxidation rate increases after 100 h of exposition. The weight increment after 204 h for the alloy AlSi28 is 0.0425 g/cm<sup>2</sup>. Nevertheless, it is apparent that at this temperature the oxidation rate of the samples covered with these layers is considerably (almost 5-times) reduced as compared with TiAl6V4 without the layer (0.209 g/cm<sup>2</sup>). The results of analyses of cuts of the layers after oxidation at 1123 K indicate that character of the original layer is almost unchanged. In the main  $\tau_2$ -phase, the content of aluminium is reduced as it diffuses to the surface and oxidizes. Formation of two sub-layers with very different contents of aluminium was observed at the interface substrate-layer. These sub-layers can be expected to have a significant effect on compactness of the layer at high temperature

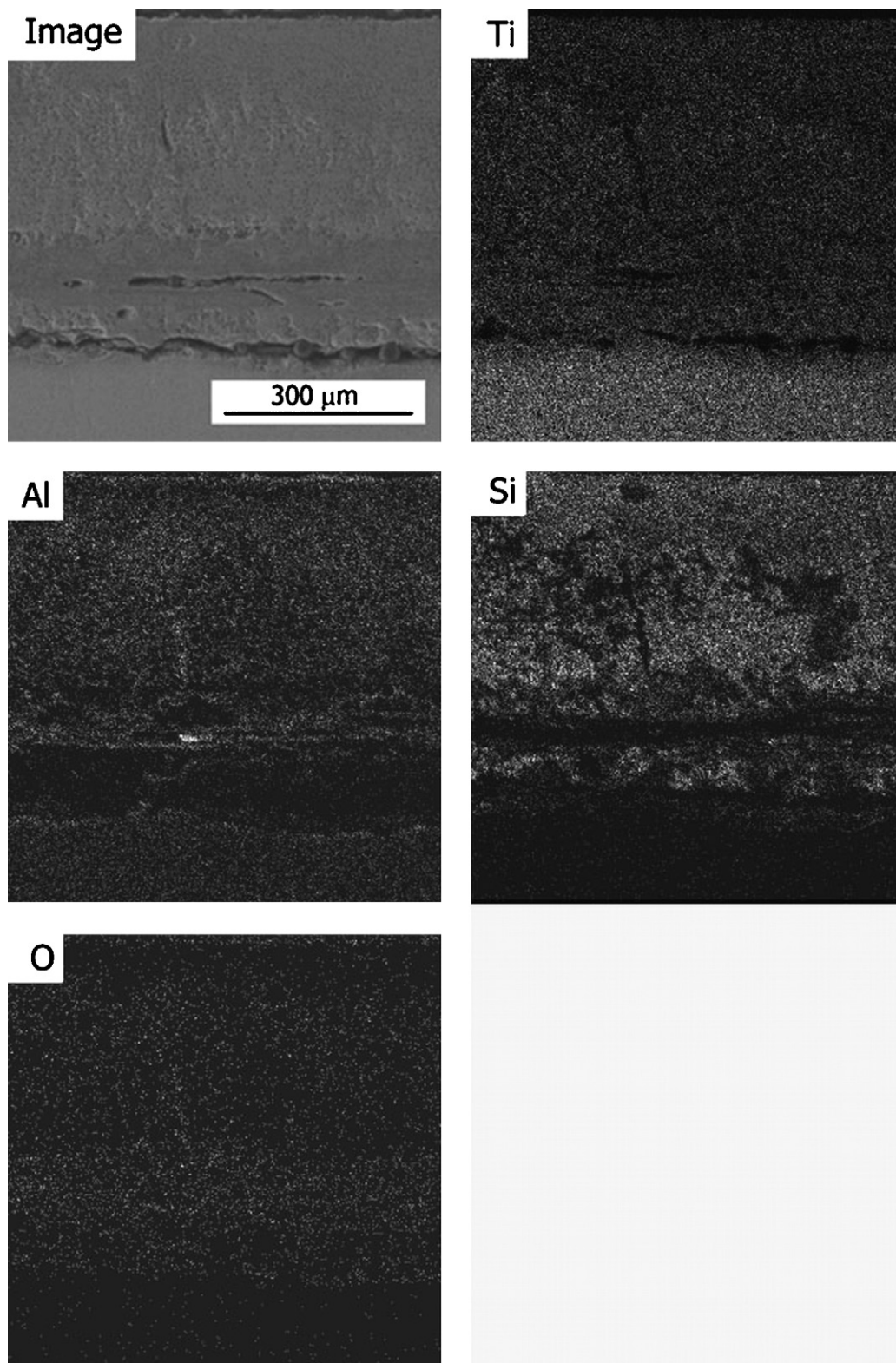


**Fig. 9.** X-ray element map of cut of the layer prepared in the melt AlSi28, oxidized at 1223 K/204 h.

gradients. Thanks to this compactness, diffusion of oxygen to the surface is also dramatically reduced.

At the oxidation temperature of 1223 K, the layers protect the substrate for up to about 100 h. Then, they flake off and the rate of oxidation and nitridation increases at the surface between the original layer and the substrate.

## 5. Conclusions

It follows from the results:

- High silicon content has a marked effect on the growth rate of the layer; using of the melt with a higher silicon con-



tent results in formation of the layer with almost a double thickness;

- It has been proved that the prepared layers protect the substrate quite efficiently against high-temperature oxidation, particularly up to the temperature of 1123 K;
- At the temperature of 1223 K, the rate of oxidation starts increasing after the 100-h exposition; practical utilization of the layers at this temperature is probably reduced; in spite of that, however, the protective efficiency of the layers remains relatively high and equals to about five-times increase in resistance as compared with the surface without the layers;
- The efficiency of the surface protection by the layers depends on the application temperature – at 1123 K, the oxidation resistance is increased about 20-times compared with the surface without the layers, whereas at 1223 K this increase is just 5-times.

## Acknowledgement

The research on surface protective layers on TiAl6V4 is financially supported by research project VZ MSM2579478701.

## References

- [1] D. Vojtěch, T. Kubatík, K. Jurek, J. Maixner, *Oxidation of Metals* 63 (2005) 305–323.
- [2] H.-P. Xiong, W. Mao, Y.-H. Xie, Wen-Li Ma, Y.-F. Chen, X.-H. Li, J.-P. Li, Y.-Y. Cheng, *Acta Materialia* 52 (2004) 2605–2620.
- [3] H.-P. Xiong, W. Mao, W.-L. Ma, Y.-H. Xie, Y.-F. Chen, H. Yuon, X.-H. Li, *Materials Science and Engineering A433* (2006) 108–113.
- [4] H.P. Xiong, Y.H. Xie, W. Mao, W.L. Ma, Y.F. Chen, X.H. Li, Y.Y. Cheng, *Scripta Materialia* 49 (2003) 1117–1122.
- [5] *Materials Science and Technology*, vol. 8. Structure and Properties of Nonferrous Alloys, VCH Verlagsgesellschaft GmbH, Weinheim, 1996.
- [6] N.S. Stoloff, C.T. Liu, S.C. Deevi, *Intermetallics* 8 (2000) 937–943.
- [7] F. Kioshi, *Emerging technology in surface modification of light metals*, *Surface and Coatings Technology* 133–134 (2000) 264–272.
- [8] A.L. Edward, *Intermetallics* 8 (2000) 1339–1345.
- [9] A. Lasalmonie, *Intermetallics* 14 (2006) 1123–1129.
- [10] L. Zhenyu, T. Narita, *Intermetallics* 12 (2004) 459–468.
- [11] D.B. Lee, S.W. Woo, *Intermetallics* 8 (2000) 1339–1345.
- [12] D. Vojtěch, J. Čížkovský, P. Novák, J. Šerák, T. Fabián, *Intermetallics* 16 (2008) 898–903.
- [13] D. Vojtěch, B. Bártová, T. Kubatík, *Materials Science and Engineering A361* (2003) 50–57.
- [14] S.O. Moussa, K. Morsi, *Journal of Alloys and Compounds* 426 (2006) 136–143.
- [15] J. Schlichting, *Ceramurgia International* 4 (1978) 162–166.
- [16] D. Vojtěch, T. Kubatík, M. Pavlíčková, J. Meixner, *Intermetallics* 14 (2006) 1181–1186.
- [17] S.E. Romankov, B.N. Mukashev, E.L. Ermakov, D.N. Muhamedshina, *Surface and Coatings Technology* 180–181 (2004) 280–285.
- [18] J. Dutta Majumdar, A. Weisheit, B.L. Mordike, I. Manna, *Materials Science and Engineering A266* (1999) 123–134.
- [19] M. Bassem, H.D. Kessler, D.J. McPherson, *Transactions of American Society for Metals* 44 (1952) 518–538.
- [20] A.M. Chaze, C. Coddet, *Oxidation of Metals* 157 (1990) 55–70.
- [21] C.L. Yeh, H.J. Wang, W.H. Chen, *Journal of Alloys and Compounds* 450 (2008) 200–207.
- [22] B. Cockeram, G. Wang, *Thin Solid Films* 269 (1995) 57–63.
- [23] J.J. Williams, Y.Y. Ye, K.M. Ho, L. Hong, C.L. Fu, S.K. Malik, *Intermetallics* 8 (2000) 937–943.
- [24] *ASM Handbook*, vol. 2. Properties and Selection: Nonferrous Alloys and Special Purpose Materials, ASM International, 1990.
- [25] P. Novák, A. Michalcová, J. Šerák, D. Vojtěch, T. Fabián, S. Randáková, F. Průša, V. Knotek, M. Novák, *Journal of Alloys and Compounds* (available online 28 March 2008).
- [26] M.H. Yoo, K. Yoshimi, *Intermetallics* 8 (2000) 1215–1224.
- [27] W. Liang, X.G. Zhao, *Scripta Materialia* 44 (2001) 1049–1054.
- [28] S.P. Gusta, *Materials Characterisation* 49 (2003) 312–330.